SANDIA REPORT
SAND2022-xxxxx
Printed April, 2022

Sandia National Laboratories

Self-Induced Curvature in an Internally Loaded Peridynamic Fiber

Stewart A. Silling

Prepared by
Sandia National Laboratories
Albuquerque, New Mexico 87185
Livermore, California 94550

Issued by Sandia National Laboratories, operated for the United States Department of Energy by National Technology & Engineering Solutions of Sandia, LLC.

Available to DOE and DOE contractors from

U.S. Department of Energy
Office of Scientific and Technical Information
P.O. Box 62
Oak Ridge, TN 37831

Telephone: (865) 576-8401
Facsimile: (865) 576-5728
E-Mail: reports@osti.gov
Online ordering: http://www.osti.gov/scitech

Available to the public from

U.S. Department of Commerce
National Technical Information Service
5301 Shawnee Road
Alexandria, VA 22312

Telephone: (800) 553-6847
Facsimile: (703) 605-6900
E-Mail: orders@ntis.gov
Online order: https://classic.ntis.gov/help/order-methods

ABSTRACT

A straight fiber with nonlocal forces that are independent of bond strain is considered. These internal loads can either stabilize or destabilize the straight configuration. Transverse waves with long wavelength have unstable dispersion properties for certain combinations of nonlocal kernels and internal loads. When these unstable waves occur, deformation of the straight fiber into a circular arc can lower its potential energy in equilibrium. The equilibrium value of the radius of curvature is computed explicitly.

CONTENTS

LIST OF FIGURES

1. INTRODUCTION

Some fibers can change length or curvature in the absence of external mechanical loading. This phenomenon affects a broad range of technologies, including paper and textiles [13, 6, 24, 1]. It is also important in artificial muscles and actuators [3, 19, 20, 9, 2, 8]. Electrospinning involves the deposition of electrostatic charge in fluids that causes them to extend into fibers. The charge continues to affect the shape and motion of the fibers after they are formed [23, 17]. In fibers that have internal structure, such as natural textile materials and optical fibers, the relative differences in properties of the constituents can induce spontaneous curvature [7].

How can the change in curvature of a fiber, without external loading, be modeled within continuum mechanics? In the present paper, nonlocal *internal loads* are introduced into a bond based peridynamic model of an initially straight fiber. These are loads that act within a bond but do not change in magnitude as the bond changes length under the deformation. Although constant in magnitude, the internal loading force density vectors rotate along with the bond as it deforms. The bond based material model does not contain explicit bending moments or rotational degrees of freedom, although these concepts have been used successfully in beam, plate, and shell models within peridynamics [14, 15, 16, 4, 25, 21, 22]. The effect of nonlocal internal loading on the stability of thin structures has apparently not been studied before. However, it is related to the phenomenon of wrinkling in thin structures caused by external loading or temperature changes, which has been investigated within peridynamics [11, 5, 10].

The main result of the present paper is that for certain combinations of the micromodulus and internal loading as they depend on bond length, a straight fiber with free ends is unstable. In these cases, an equilibrium curvature can be computed explicitly.

In the remainder of the paper, Section 2 considers the dynamic stability of the straight nonlocal fiber with respect to transverse wave motion. In Section 3, approximations for the strain energy in a fiber are derived as a function of axial strain and curvature. In Section 4, the equilibrium curvature and self-shaping in a fiber with free ends is discussed. Conclusions are presented in Section 5.

2. TRANSVERSE WAVES

Among the simplest examples of wave motion is the transverse vibration of a string under tension. In this section, the peridynamic version of this elementary problem is considered, including internal loading. (These waves are referred to here as *transverse waves* rather than "bending waves" to avoid confusion with the use of the latter term in beam and plate theory.)

Consider a long, thin peridynamic body whose undeformed configuration is a long interval on the x_1-axis and whose cross-sectional area is a (Figure 2-1). a is small enough that in the absence of internal loading, the body has negligible resistance to bending. (Background on the peridynamic theory is available in the book by Madenci and Oterkus [12].) Let $\mathbf{y}$ denote the deformation map and $\mathbf{u}$ the displacement vector,

$$\mathbf{y}(\mathbf{x},t) = \mathbf{x} + \mathbf{u}(\mathbf{x},t). \tag{1}$$

Let $u_2(x_1,t)$ denote the transverse deflection, which is assumed to be small. For a given bond $\boldsymbol{\xi} = \mathbf{e}_1\xi$, let p be the deformed bond length (Figure 2-2),

$$p = |\mathbf{y}(\mathbf{x}+\boldsymbol{\xi},t) - \mathbf{y}(\mathbf{x},t)|. \tag{2}$$

Let s be the bond strain,

$$s = \frac{p}{|\boldsymbol{\xi}|} - 1. \tag{3}$$

The deformed bond direction vector is denoted by $\mathbf{M}$:

$$\mathbf{M} = \frac{\mathbf{y}(\mathbf{x}+\boldsymbol{\xi},t) - \mathbf{y}(\mathbf{x},t)}{p}. \tag{4}$$

The peridynamic equation of motion in three dimensions is given by

$$\rho\ddot{\mathbf{u}}(\mathbf{x},t) = \int_{\mathscr{H}_\mathbf{x}} \mathbf{f}(\mathbf{x}+\boldsymbol{\xi},\mathbf{x},t)\,\mathrm{d}\boldsymbol{\xi} + \mathbf{b}(\mathbf{x},t) \tag{5}$$

where ρ is the density, $\mathscr{H}_\mathbf{x}$ is a neighborhood of $\mathbf{x}$ called the *family* of $\mathbf{x}$, and $\mathbf{b}$ is the external body force density, which throughout the remainder of this paper will be assumed to equal zero. The vector valued function $\mathbf{f}$ is the pairwise bond force density, which is determined by the deformation through the material model. In the present case of the thin fiber initially on the x_1-axis, (5) is approximated by

$$\rho\ddot{\mathbf{u}}(\mathbf{x},t) = a\int_{-\delta}^{\delta} \mathbf{f}(x_1+\xi,x_1,t)\,\mathrm{d}\xi \tag{6}$$

where δ is the horizon. Throughout this discussion, three-dimensional material models are used for purposes of units.

Suppose the material model is microelastic with micropotential given by

$$w(p,\xi) = \frac{c(\xi)}{2}|\xi|s^2 + f_i(\xi)|\xi|s \tag{7}$$

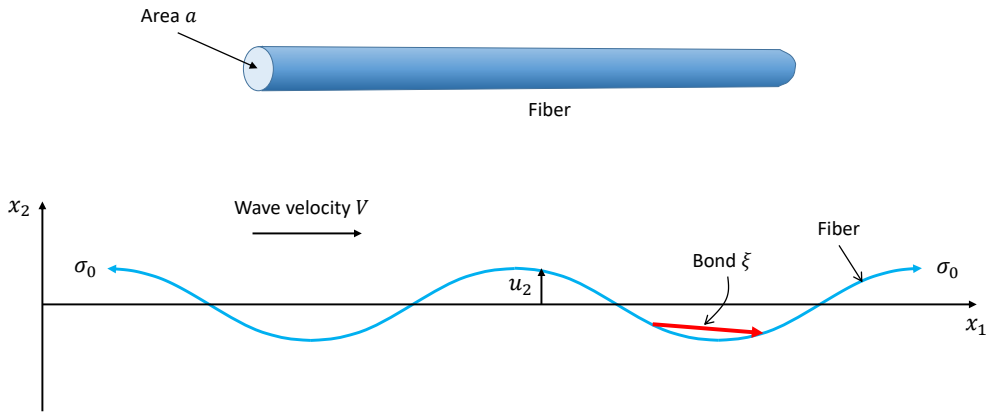

Figure 2-1 Transverse wave in a nonlocal fiber with axial stress σ_0.

Figure 2-2 Undeformed and deformed bond in a fiber model.

where s is given by (3) and c is the micromodulus, which is assumed to be positive on $(0,\delta]$. In (7), f_i is the bond's *internal load*, which depends on ξ but not on x_1 or on s. Assume that c and f_i are symmetric:

$$c(-\xi) = c(\xi), \qquad f_i(-\xi) = f_i(\xi) \tag{8}$$

for all ξ. From (7), the pairwise bond force density is given by

$$\mathbf{f}(x_1+\xi, x_1, t) = \hat{f}(s,\xi)\mathbf{M} \tag{9}$$

where

$$\hat{f}(s,\xi) = \frac{\partial w}{\partial p}(p,\xi) = c(\xi)s + f_i(\xi). \tag{10}$$

In the following discussion, the subscript 0 refers to an initial, straight configuration of the fiber. Suppose that initially the (straight) fiber has a constant strain ε_0, which can be due to remote loading or internal loading. Define the initial stretch by

$$\lambda_0 = 1 + \varepsilon_0. \tag{11}$$

The (normal) stress σ_0 in the fiber is found from the partial stress tensor [18], which in the present case simplifies to

$$\sigma_0 = a\int_0^\delta \hat{f}(\varepsilon_0,\xi)\xi \, \mathrm{d}\xi. \tag{12}$$

In (12), σ_0 has dimensions of force/area, as in 3D. From (10) and (12),

$$\sigma_0 = a\int_0^\delta (c(\xi)\varepsilon_0 + f_i(\xi))\xi \, \mathrm{d}\xi. \tag{13}$$

From (13), it follows that the Young's modulus is given by

$$E = \frac{\mathrm{d}\sigma_0}{\mathrm{d}\varepsilon_0} = a\int_0^\delta c(\xi)\xi \, \mathrm{d}\xi. \tag{14}$$

To investigate the propagation of transverse waves in the nonlocal fiber with internal loading, the dispersion properties of these waves will now be derived. For a bond ξ, under the assumption of small deflections,

$$M_2 = \frac{u_2(x_1+\xi,t) - u_2(x_1,t)}{|\xi|}. \tag{15}$$

From (9) and (15),

$$f_2(x_1+\xi, x_1, t) = \frac{f_0(\xi)}{|\xi|}(u_2(x_1+\xi,t) - u_2(x_1,t)) \tag{16}$$

where, from (10),

$$f_0(\xi) := \hat{f}(\varepsilon_0,\xi) = c(\xi)\varepsilon_0 + f_i(\xi). \tag{17}$$

Assume a transverse wave of the form

$$u_2(x) = e^{i(kx-\omega t)} \tag{18}$$

where k is the wavenumber and ω is the angular frequency. The equation of motion (6) reduces to

$$\rho \ddot{u}_2(\mathbf{x},t) = a \int_{-\delta}^{\delta} f_2(x_1+\xi, x_1, t)\, \mathrm{d}\xi. \tag{19}$$

Using (16), (17), and (19), differentiating (18) twice with respect to time leads to

$$\rho \omega^2 = a \int_{-\delta}^{\delta} \frac{f_0(\xi)}{|\xi|} \left(1 - e^{ik\xi}\right)\, \mathrm{d}\xi. \tag{20}$$

Since the integrand in (20) is an even function,

$$\rho \omega^2(k) = 2a \int_0^{\delta} \frac{f_0(\xi)}{\xi} \left(1 - \cos(k\xi)\right)\, \mathrm{d}\xi. \tag{21}$$

Equation (21) is the dispersion relation for transverse waves. If $\omega^2(k) > 0$ for all $k > 0$, then the system is stable in the sense of propagating waves of constant amplitude with any wavenumber. If $\omega^2(k) \geq 0$ for all $k > 0$ but $\omega^2(k_0) = 0$ for some $k_0 > 0$, then the system is neutrally stable. If $\omega^2(k) < 0$ for some $k_0 > 0$, then the system is unstable.

To study the stability of long waves, it suffices to derive the leading terms in (21) for small k. Using the first few terms of a Taylor series for cosine in (21) leads to

$$\rho \omega^2(k) = 2a \int_0^{\delta} \frac{f_0(\xi)}{\xi} \left(\frac{k^2\xi^2}{2} - \frac{k^4\xi^4}{24} + O(k^6)\right)\, \mathrm{d}\xi. \tag{22}$$

Combining (13), (17), and (22), and neglecting terms of order k^6 or higher,

$$\rho \omega^2(k) = \sigma_0 k^2 - B k^4, \qquad |k| \ll 1/\delta \tag{23}$$

where

$$B = \frac{a}{12} \int_0^{\delta} (c(\xi)\varepsilon_0 + f_i(\xi))\xi^3\, \mathrm{d}\xi. \tag{24}$$

To obtain the phase velocity, which is defined by $V(k) = \omega/k$, (23) implies

$$V(k) = \sqrt{\frac{\sigma_0 - Bk^2}{\rho}}, \qquad |k| \ll 1/\delta. \tag{25}$$

The terms involving B in (23) and (25) incorporate the effect of nonlocality and internal loading.

Now restrict attention to the case of a fiber with free ends, so that

$$\sigma_0 = 0. \tag{26}$$

In this case, from (13) and (26),

$$\varepsilon_0 = \varepsilon_{free} := -\frac{\int_0^{\delta} f_i(\xi)\xi\, \mathrm{d}\xi}{\int_0^{\delta} c(\xi)\xi\, \mathrm{d}\xi} \tag{27}$$

and from (23),

$$\rho\omega^2(k) = -Bk^4. \tag{28}$$

Therefore, in the case of a fiber with free ends, the system is unstable if

$$B > 0. \tag{29}$$

An example of the effect of internal loading on the dispersion curve of a fiber is illustrated in Figure 2-3. In this example, a long fiber has a material model given by

$$c(\xi) = 1, \qquad f_i(\xi) = \eta + \beta\left(\frac{\xi}{\delta} - \frac{2}{3}\right) \tag{30}$$

where η and β are constants. The effect of β is to change whether the internal loading in long bonds is more tensile ($\beta > 0$) or more compressive ($\beta < 0$) than short bonds. For the fiber with free ends, (27) and (30) lead to

$$\varepsilon_0 = \varepsilon_{free} = -\eta. \tag{31}$$

Using (24) and (31),

$$B = \frac{a\delta^4}{360}\beta. \tag{32}$$

So, comparing (28) and (32), the fiber is unstable if $\beta > 0$, that is, if longer bonds have more tensile internal loading than shorter bonds. Perhaps surprisingly, η has no effect on stability, since it does not appear in (32). This observation does not necessarily hold if a different form of $c(\xi)$ is used.

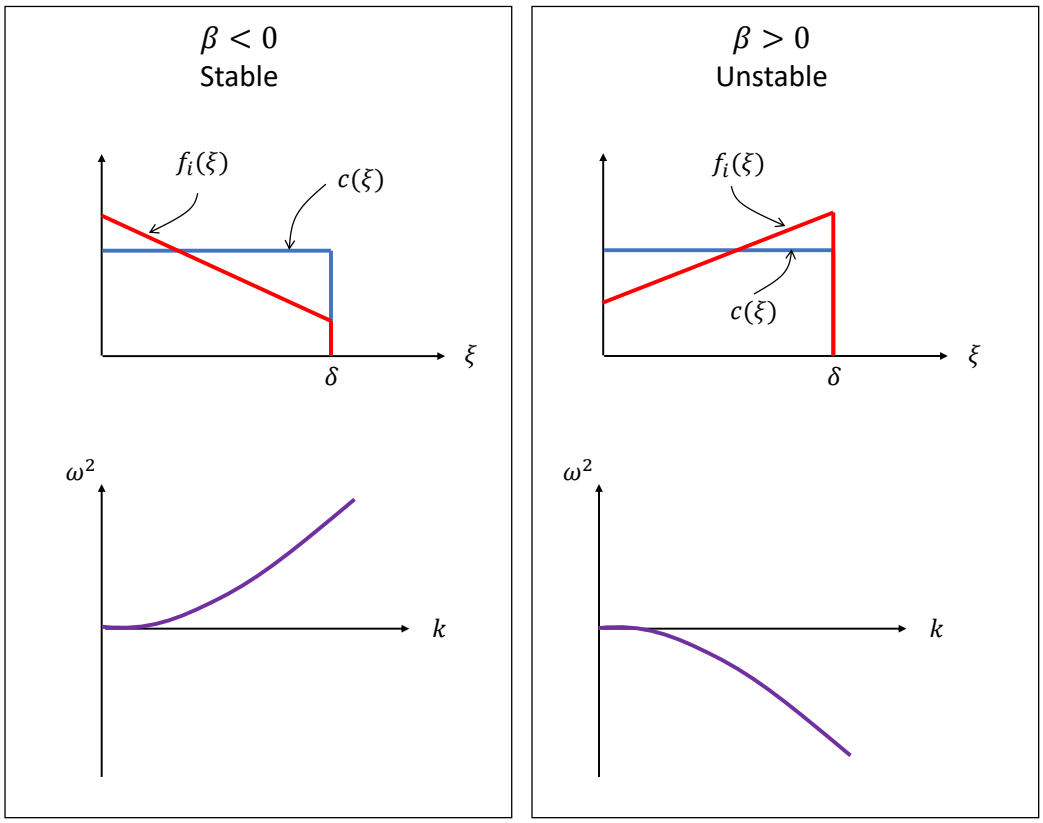

Figure 2-3 Stable and unstable forms of the material model in (30)**. Top: material models. Bottom: dispersion curves.**

3. POTENTIAL ENERGY IN A FIBER WITH CONSTANT CURVATURE

The previous section showed that a fiber with internal loading can be either stable or unstable in the straight configuration. The remainder of this paper concerns the equilibrium configuration of a fiber, particularly in the event that the straight configuration is unstable. To investigate this, the potential energy in a family of deformations parameterized by curvature and tangential (axial) strain will be derived.

Suppose the straight fiber has strain ε_0, so the stretch is $\lambda_0 = 1 + \varepsilon_0$. The fiber then undergoes a further incremental deformation such that its deformed radius of curvature is a constant r. The tangential strain also incrementally changes by ε in this additional deformation. The final tangential stretch λ is therefore

$$\lambda = \lambda_0 + \varepsilon. \tag{33}$$

Referring to Figure 3-1, the deformed bond length of a bond ξ is given by

$$p = 2r \sin\frac{\theta}{2}, \qquad \theta = \frac{\lambda|\xi|}{r}. \tag{34}$$

To simplify the algebra, without loss of generality, assume $\xi > 0$. From (3) and (34), the bond strain is given by

$$s = \frac{2r}{\xi} \sin\left(\frac{\lambda\xi}{2r}\right) - 1. \tag{35}$$

To obtain the leading terms in (35), use the first few terms of the Taylor series for sine,

$$\sin z = z - \frac{z^3}{6} + \frac{z^5}{120} + O(z^7). \tag{36}$$

From (35) and (36),

$$s = \frac{2r}{\xi}\left[\left(\frac{\lambda\xi}{2r}\right) - \frac{1}{6}\left(\frac{\lambda\xi}{2r}\right)^3 + \frac{1}{120}\left(\frac{\lambda\xi}{2r}\right)^5 + O((\delta/r)^7)\right] - 1. \tag{37}$$

Simplifying (37) leads to

$$s = (\lambda - 1) - \frac{\lambda^3\xi^2}{24r^2} + \frac{\lambda^5\xi^4}{1920r^4} + O((\delta/r)^6) \tag{38}$$

Using (11) and (33), (38) becomes

$$s = \varepsilon_0 + \varepsilon - \frac{(\lambda_0+\varepsilon)^3\xi^2}{24r^2} + \frac{(\lambda_0+\varepsilon)^5\xi^4}{1920r^4} + O((\delta/r)^6). \tag{39}$$

Expanding the powers of $\lambda_0 + \varepsilon$ in (39) leads to

$$s = \varepsilon_0 + \varepsilon - \frac{(\lambda_0^3 + 3\lambda_0^2\varepsilon)\xi^2}{24r^2} + \frac{(\lambda_0^5 + 5\lambda_0^4\varepsilon)\xi^4}{1920r^4} + O((\delta/r)^6) + O(\varepsilon\delta/r)^2). \tag{40}$$

Let ψ denote the curvature of the fiber, defined by

$$\psi = \frac{1}{r}. \tag{41}$$

Because the lowest order term that depends on curvature in (40) involves ψ^2 rather than ψ, it is convenient to work with κ defined by

$$\kappa = \psi^2 = \frac{1}{r^2}. \tag{42}$$

From (40) and (42),

$$s = \varepsilon_0 + \varepsilon - \frac{(\lambda_0^3 + 3\lambda_0^2\varepsilon)\kappa\xi^2}{24} + \frac{(\lambda_0^5 + 5\lambda_0^4\varepsilon)\kappa^2\xi^4}{1920} + O((\delta^2\kappa)^3) + O(\varepsilon^2\delta^2\kappa)). \tag{43}$$

Retaining terms up to second order (that is, up to and including ε^2, κ^2, and $\varepsilon\kappa$), (43) yields

$$s = \varepsilon_0 + \varepsilon - \frac{\lambda_0^3\xi^2}{24}\kappa + \frac{\lambda_0^5\xi^4}{1920}\kappa^2 - \frac{\lambda_0^2\xi^2}{8}\varepsilon\kappa. \tag{44}$$

Taking the square of (44) and discarding the higher order terms leads to

$$s^2 = \varepsilon_0^2 + 2\varepsilon_0\varepsilon - \frac{\varepsilon_0\lambda_0^3\xi^2}{12}\kappa + \varepsilon^2 + \left(\frac{\lambda_0^6\xi^4}{576} + \frac{\varepsilon_0\lambda_0^5\xi^4}{960}\right)\kappa^2 + \left(-\frac{\lambda_0^3\xi^2}{12} - \frac{\varepsilon_0\lambda_0^2\xi^2}{4}\right)\varepsilon\kappa. \tag{45}$$

Now that we have explicit expressions for s and s^2 in terms of κ and ε given by (44) and (45), the bond micropotential is evaluated using (7) to give

$$\begin{aligned} w(\varepsilon,\kappa,\xi) = \frac{c(\xi)}{2}\xi \Bigg[& \varepsilon_0^2 + 2\varepsilon_0\varepsilon - \frac{\varepsilon_0\lambda_0^3\xi^2}{12}\kappa + \varepsilon^2 \\ & + \left(\frac{\lambda_0^6\xi^4}{576} + \frac{\varepsilon_0\lambda_0^5\xi^4}{960}\right)\kappa^2 + \left(-\frac{\lambda_0^3\xi^2}{12} - \frac{\varepsilon_0\lambda_0^2\xi^2}{4}\right)\varepsilon\kappa \Bigg] \\ & + f_i(\xi)\xi\left[\varepsilon_0 + \varepsilon - \frac{\lambda_0^3\xi^2}{24}\kappa + \frac{\lambda_0^5\xi^4}{1920}\kappa^2 - \frac{\lambda_0^2\xi^2}{8}\varepsilon\kappa\right]. \end{aligned} \tag{46}$$

The strain energy density is given by

$$W = \frac{a}{2}\int_{-\delta}^{\delta} w(\varepsilon,\kappa,\xi)\,\mathrm{d}\xi. \tag{47}$$

From (46) and (47),

$$W = W_0 + \sigma_0\varepsilon - A_1\kappa + A_2\varepsilon^2 + A_3\kappa^2 - A_4\varepsilon\kappa \tag{48}$$

where σ_0 is given by (13) and

$$\begin{aligned}
W_0 &= a\varepsilon_0 \int_0^\delta \left[\frac{c(\xi)}{2}\varepsilon_0 + f_i(\xi)\right] \xi \, \mathrm{d}\xi, \\
A_1 &= \frac{a\lambda_0^3}{24} \int_0^\delta \left[c(\xi)\varepsilon_0 + f_i(\xi)\right] \xi^3 \, \mathrm{d}\xi, \\
A_2 &= \frac{a}{2} \int_0^\delta c(\xi)\xi \, \mathrm{d}\xi = \frac{E}{2}, \\
A_3 &= \frac{a\lambda_0^5}{1920} \int_0^\delta \left[c(\xi)\left(\frac{5\lambda_0}{3} + \varepsilon_0\right) + f_i(\xi)\right] \xi^5 \, \mathrm{d}\xi, \\
A_4 &= \frac{a\lambda_0^2}{8} \int_0^\delta \left[c(\xi)\left(\frac{\lambda_0}{3} + \varepsilon_0\right) + f_i(\xi)\right] \xi^3 \, \mathrm{d}\xi.
\end{aligned} \tag{49}$$

Figure 3-2 shows the strain energy density given by (48) and (49) as a function of curvature for the material with $\eta = 0$ and $\beta = 0.02$, arbitrarily setting $\varepsilon = 0.02$ for purposes of illustration. This expression is approximate because it retains terms in the bond strain only up to second order, as discussed above. For comparison, the figure also shows the exact result, which is obtained by combining (7), (35), and (47).

The total potential energy Φ will be used in the next section to investigate the equilibrium configuration of the fiber. This is found by integrating W over volume, therefore

$$\Phi(\kappa) = LaW \tag{50}$$

where L is the length of the fiber. (48) and (50) lead to

$$\Phi(\kappa, \varepsilon) = La\big(W_0 + \sigma_0\varepsilon - A_1\kappa + A_2\varepsilon^2 + A_3\kappa^2 - A_4\varepsilon\kappa\big). \tag{51}$$

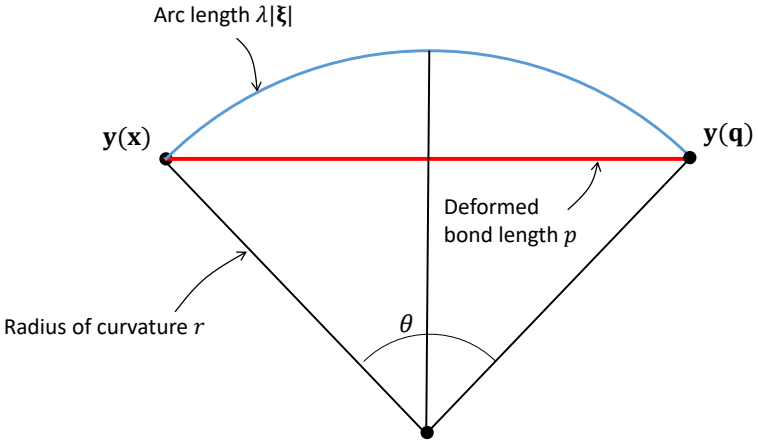

Figure 3-1 In a curved fiber, p is the deformed length of the bond $\boldsymbol{\xi}$.

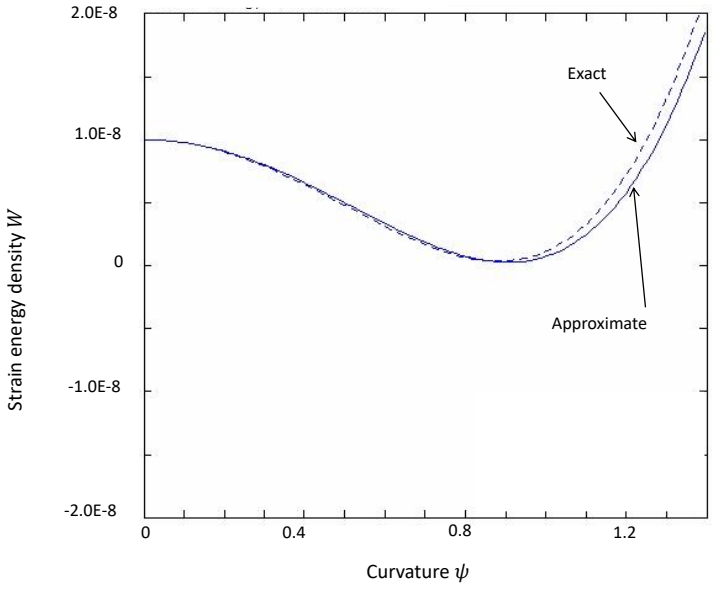

Figure 3-2 Strain energy density as a function of curvature with a typical set of material parameters.

4. FIBER WITH FREE ENDS

Consider an initially straight fiber of length L, with $L \gg \delta$. Suppose the ends are free, so that the stress in the straight configuration is given by

$$\sigma_0 = 0. \tag{52}$$

There can be a nonzero value of λ_0, which is found from (27), thus

$$\lambda_0 = 1 + \varepsilon_0, \qquad \varepsilon_0 = \varepsilon_{free}. \tag{53}$$

To minimize the potential energy given by (51), set

$$\begin{aligned} 0 &= \frac{\partial \Phi}{\partial \varepsilon} = La(2A_2\varepsilon - A_4\kappa), \\ 0 &= \frac{\partial \Phi}{\partial \kappa} = La(-A_1 + 2A_3\kappa - A_4\varepsilon), \qquad \kappa > 0. \end{aligned} \tag{54}$$

Solving (54) for the equilibrium values of κ and ε yields

$$\kappa_{eq} = \max\left\{0, \frac{2A_1A_2}{4A_2A_3 - A_4^2}\right\}, \qquad \varepsilon_{eq} = \frac{A_4\kappa_{eq}}{2A_2}. \tag{55}$$

Using the third equation of (49), (55) can be rewritten in the slightly more suggestive form

$$\kappa_{eq} = \max\left\{0, \frac{EA_1}{2EA_3 - A_4^2}\right\}, \qquad \varepsilon_{eq} = \frac{A_4\kappa_{eq}}{E}. \tag{56}$$

The denominator $2EA_3 - A_4^2$ in the first equation of (56) is positive for sufficiently small f_i (see Appendix). The fiber length L has no effect on the curvature of the fiber.

An example of the self-induced curvature of a fiber with free ends is shown in Figure 4-1. In this example, δ=1 and a=1.0E-4. The material model is given by (30). Three cases with different values of η are shown, with β on the horizontal axis. The plots show that for $\beta < 0$ (less tensile internal loading in the long bonds) the fiber remains straight. As β becomes positive (more tensile internal loading in long bonds), the curvature rises rapidly. As the curvature increases, the axial stretch also shows a modest increase.

Comparing (24) with the second equation of (49), evidently

$$A_1 = \frac{\lambda_0^3 B}{2}. \tag{57}$$

Therefore, when the straight fiber is unstable in the sense of imaginary wave speeds according to the condition (29), the result (56) shows that a curved shape is stable in the sense of energy minimization. Conversely, when there is stable wave propagation, the straight configuration is the energy minimizer. These observations establish the connection between unstable waves and self-induced curvature.

It is interesting to compute the resistance of the fiber with self-induced curvature to further changes in curvature. During these increments in curvature, the energy is stationary with respect to changes in ε, so the first equation of (54) continues to hold, and therefore

$$\varepsilon = \frac{A_4}{2A_2}\kappa. \tag{58}$$

Next, combine (51), (52), and (58) to obtain

$$\frac{\Phi}{La} = W_0 - A_1\kappa + \left[A_2\left(\frac{A_4}{2A_2}\right)^2 + A_3 - A_4\left(\frac{A_4}{2A_2}\right)\right]\kappa^2. \tag{59}$$

Using (42) and rearranging, (59) leads to

$$\frac{\Phi}{La} = W_0 - A_1\psi^2 + \left[A_3 - \frac{A_4^2}{4A_2}\right]\psi^4. \tag{60}$$

The resistance of the fiber to changes in curvature can be defined by

$$S(\psi) = \frac{1}{2La}\frac{\mathrm{d}^2\Phi}{\mathrm{d}\psi^2}. \tag{61}$$

From (60) and (61),

$$S(\psi) = -A_1 + 6\left[A_3 - \frac{A_4^2}{4A_2}\right]\psi^2. \tag{62}$$

Evaluating (62) at $\psi_{eq}^2 = \kappa_{eq}$ using the first of (55) yields

$$\begin{aligned} S(\psi_{eq}) &= -A_1 + 6\left[A_3 - \frac{A_4^2}{4A_2}\right]\frac{2A_1A_2}{4A_2A_3 - A_4^2} \\ &= 2A_1. \end{aligned} \tag{63}$$

Recall that $A_1 > 0$ is the condition for instability in the straight fiber. So, (63) suggests that as material parameters such as β change to cause A_1 to increase and therefore make the system "more unstable," the curved, stable configuration becomes stiffer with respect to further increments in curvature.

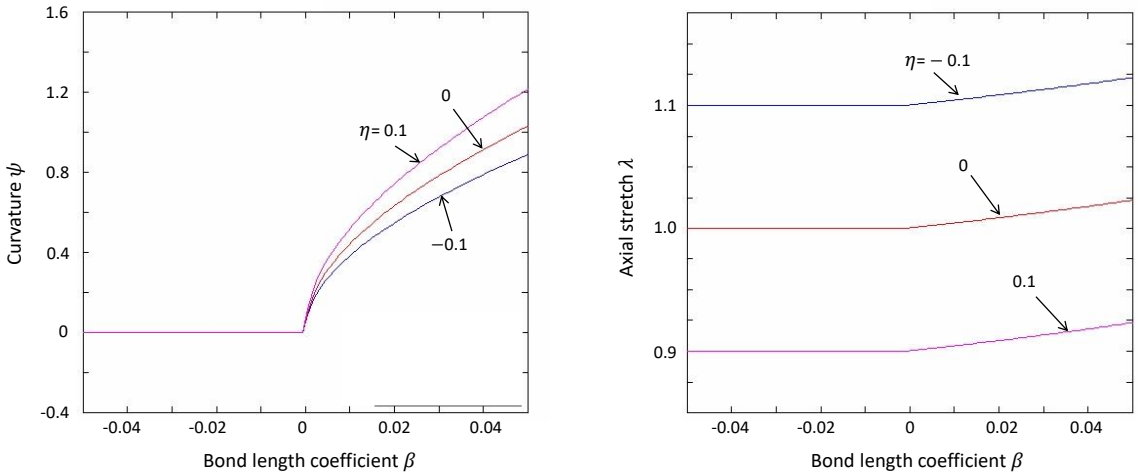

Figure 4-1 Self-induced curvature and strain in a fiber with free ends as a function of β in the material model (30). $\beta > 0$ means that long bonds have tensile internal load, while short bonds have compressive internal load.

5. CONCLUSIONS

The main result of this paper is that internal loading can either stabilize or destabilize an initially straight fiber with free ends. This instability is reflected in the sign of the dispersion relation for certain combinations of the functions c and f_i, as stated in equations (24) and (29). It is also reflected in the fact that the straight configuration can be a local maximum, rather than a local minimum, in the potential energy of the system. In these cases, the equilibrium curvature of a local minimizer can be computed explicitly.

The unstable behavior of a fiber with nonlocal internal loading in some ways resembles the classical problem of the buckling of an elastic beam under prescribed compressive loading at the ends, since both result in the spontaneous appearance of curvature. However, in the case of the nonlocal fiber, there is apparently only one equilibrium value of curvature, whereas in the beam buckling problem the final curvature is undetermined.

This paper does not address the question of how to find a configuration that is a *global* minimizer, which appears to be a very challenging problem that resembles that of protein folding. The present results also do not prove, or even suggest, that the circular arc is necessarily obtained as a large-time solution for arbitrarily shaped initial conditions in a time-dependent model. For example, an initially tangled fiber could stay tangled. The present results only establish that a curved fiber can have lower energy than a straight fiber, depending on the choice of c and f_i.

Thermal expansion with a coefficient of thermal expansion (CTE) α that depends on bond length provides an example of nonlocal internal loading. In this case, the internal loading is simply given by $f_i(\xi) = -\alpha(\xi)c(\xi)(T - T_0)$, where T is the current temperature and T_0 is room temperature. Based on the results in the present paper, a fiber with free ends composed of such a material could change from straight to curved and back again, depending on the current temperature. Similar bond-length dependence in the nonlocal material model could be used to model the effects of moisture, electrostatic charge, or other environmental factors.

REFERENCES

[1] A. Brandberg, H. R. Motamedian, A. Kulachenko, and U. Hirn. The role of the fiber and the bond in the hygroexpansion and curl of thin freely dried paper sheets. *International Journal of Solids and Structures*, 193:302–313, 2020.

[2] H. Chen, D. F. Baptista, G. Criscenti, J. Crispim, H. Fernandes, C. Van Blitterswijk, R. Truckenmüller, and L. Moroni. From fiber curls to mesh waves: A platform for the fabrication of hierarchically structured nanofibers mimicking natural tissue formation. *Nanoscale*, 11(30):14312–14321, 2019.

[3] H. Cheng, J. Liu, Y. Zhao, C. Hu, Z. Zhang, N. Chen, L. Jiang, and L. Qu. Graphene fibers with predetermined deformation as moisture-triggered actuators and robots. *Angewandte Chemie International Edition*, 52(40):10482–10486, 2013.

[4] S. R. Chowdhury, P. Roy, D. Roy, and J. Reddy. A peridynamic theory for linear elastic shells. *International Journal of Solids and Structures*, 84:110–132, 2016.

[5] C. Diyaroglu, D. Behera, E. Madenci, Y. Kaya, G. Kedziora, and D. Nepal. Peridynamic modeling of wrinkling in a graphene layer. In *AIAA Scitech 2019 Forum*, page 1040, 2019.

[6] J. Gärd. The influence of fibre curl on the shrinkage and strength properties of paper, thesis, University of Technology, Lulea, Sweden, 2002.

[7] J. W. Hearle. The structural mechanics of fibers. *Journal of Polymer Science Part C: Polymer Symposia*, 20(1):215–251, 1967.

[8] Z. Hu, Y. Li, and J. Lv. Phototunable self-oscillating system driven by a self-winding fiber actuator. *Nature Communications*, 12(1):1–9, 2021.

[9] H. Kim, J. H. Moon, T. J. Mun, T. G. Park, G. M. Spinks, G. G. Wallace, and S. J. Kim. Thermally responsive torsional and tensile fiber actuator based on graphene oxide. *ACS Applied Materials and Interfaces*, 10(38):32760–32764, 2018.

[10] M. Laurien, A. Javili, and P. Steinmann. Nonlocal wrinkling instabilities in bilayered systems using peridynamics. *Computational Mechanics*, pages 1–15, 2021.

[11] H. Li, Y. Zheng, Y. Zhang, H. Ye, and H. Zhang. Large deformation and wrinkling analyses of bimodular structures and membranes based on a peridynamic computational framework. *Acta Mechanica Sinica*, 35(6):1226–1240, 2019.

[12] E. Madenci and E. Oterkus. *Peridynamic Theory and Its Applications*. Springer, New York, 2013.

[13] U.-B. Mohlin and C. Alfredsson. Fibre deformation and its implications in pulp characterization. *Nordic Pulp & Paper Research Journal*, 5(4):172–179, 1990.

[14] J. O'Grady and J. Foster. Peridynamic beams: a non-ordinary, state-based model. *International Journal of Solids and Structures*, 51(18):3177–3183, 2014.

[15] J. O'Grady and J. Foster. Peridynamic plates and flat shells: A non-ordinary, state-based model. *International Journal of Solids and Structures*, 51(25-26):4572–4579, 2014.

[16] J. O'Grady and J. Foster. A meshfree method for bending and failure in non-ordinary peridynamic shells. *Computational Mechanics*, 57(6):921–929, 2016.

[17] C.-L. Pai, M. C. Boyce, and G. C. Rutledge. On the importance of fiber curvature to the elastic moduli of electrospun nonwoven fiber meshes. *Polymer*, 52(26):6126–6133, 2011.

[18] S. Silling, D. Littlewood, and P. Seleson. Variable horizon in a peridynamic medium. *Journal of Mechanics of Materials and Structures*, 10(5):591–612, 2015.

[19] N. Sinatra, T. Ranzani, J. Vlassak, K. Parker, and R. Wood. Nanofiber-reinforced soft fluidic micro-actuators. *Journal of Micromechanics and Microengineering*, 28(8):084002, 2018.

[20] X. Yang, W. Wang, and M. Miao. Moisture-responsive natural fiber coil-structured artificial muscles. *ACS Applied Materials and Interfaces*, 10(38):32256–32264, 2018.

[21] Z. Yang, E. Oterkus, C. T. Nguyen, and S. Oterkus. Implementation of peridynamic beam and plate formulations in finite element framework. *Continuum Mechanics and Thermodynamics*, 31(1):301–315, 2019.

[22] Z. Yang, E. Oterkus, and S. Oterkus. Peridynamic higher-order beam formulation. *Journal of Peridynamics and Nonlocal Modeling*, 3(1):67–83, 2021.

[23] A. L. Yarin, S. Koombhongse, and D. H. Reneker. Bending instability in electrospinning of nanofibers. *Journal of Applied Physics*, 89(5):3018–3026, 2001.

[24] X. Zeng, S. Fu, E. Retulainen, and S. Heinemann. Fibre deformations induced by different mechanical treatments and their effect on zero-span strength. *Nordic Pulp & Paper Research Journal*, 27(2):335–342, 2012.

[25] Q.-Z. Zhu and T. Ni. Peridynamic formulations enriched with bond rotation effects. *International Journal of Engineering Science*, 121:118–129, 2017.

APPENDIX

Here, it is shown that for sufficiently small f_i, the denominator in the first of (56) is positive. Suppose $f_i \equiv 0$, which implies that $\varepsilon_0 = 0$ and $\lambda_0 = 1$. Recall that $c > 0$ by assumption. Then using (14) and (49), write the denominator in the first of (56) as

$$D := 2EA_3 - A_4^2$$
$$= a^2 \left(2 \int_0^\delta c(x) x \, \mathrm{d}x \right) \left(\int_0^\delta \frac{c(x)x^5}{1152} \, \mathrm{d}x \right) - a^2 \left(\int_0^\delta \frac{c(x)x^5}{24} \, \mathrm{d}x \right)^2 . \quad (64)$$

Shortening the notation slightly, and changing the dummy variable of integration, (64) yields

$$\begin{aligned}
\frac{576D}{a^2} &= \int c(x)x \int c(y)y^5 - \int c(x)x^3 \int c(y)y^3 \\
&= \int\int c(x)c(y)(xy^5 - x^3y^3) \\
&= \int\int c(x)c(y)(xy)y^2(y^2 - x^2) \\
&= \frac{1}{2}\int\int c(x)c(y)(xy)y^2(y^2 - x^2) \\
&\qquad + \frac{1}{2}\int\int c(y)c(x)(yx)x^2(x^2 - y^2) \\
&= \frac{1}{2}\int\int c(x)c(y)(xy)y^2(y^2 - x^2) \\
&\qquad - \frac{1}{2}\int\int c(y)c(x)(yx)x^2(y^2 - x^2) \\
&= \frac{1}{2}\int\int c(x)c(y)(xy)(y^2 - x^2)^2
\end{aligned}$$

where the dummy variables x and y are interchanged in the fourth line. Since the integrand in the last line is positive for all x and y except on the line $x = y$, this proves that $D > 0$ for $f_i \equiv 0$. Therefore this result must also be true for sufficiently small f_i.

DISTRIBUTION

Hardcopy—External

Number of Copies	Name(s)	Company Name and Company Mailing Address

Hardcopy—Internal

Number of Copies	Name	Org.	Mailstop

Email—Internal [redacted]

Name	Org.	Sandia Email Address
Technical Library	01177	libref@sandia.gov

Sandia National Laboratories

Sandia National Laboratories is a multimission laboratory managed and operated by National Technology & Engineering Solutions of Sandia LLC, a wholly owned subsidiary of Honeywell International Inc., for the U.S. Department of Energy's National Nuclear Security Administration under contract DE-NA0003525.